Numerical and analytical investigation of the synchronization of dipolarly coupled vortex spin-torque nano-oscillators

A. D. Belanovsky,[1] N. Locatelli,[2] P. N. Skirdkov,[1] F. Abreu Araujo,[3] K. A. Zvezdin,[1,4,a)] J. Grollier,[2] V. Cros,[2] and A. K. Zvezdin[1]
[1]*A. M. Prokhorov General Physics Institute, RAS, Vavilova, 38, 119991 Moscow and Russia and Moscow Institute of Physics and Technology, Institutskiy per. 9, 141700 Dolgoprudny, Russia*
[2]*Unité Mixte de Physique CNRS/Thales, 1 ave A. Fresnel, 91767 Palaiseau, and Univ Paris-Sud, 91405 Orsay, France*
[3]*Université catholique de Louvain, 1 Place de l'Université, 1348 Louvain-la-Neuve, Belgium*
[4]*Istituto P.M. srl, via Grassi, 4, 10138 Torino, Italy*

(Received 5 August 2013; accepted 28 August 2013; published online 18 September 2013)

We investigate analytically and numerically the synchronization dynamics of dipolarly coupled vortex based Spin-Torque Nano Oscillators with different pillar diameters. We identify the critical interpillar distances on which synchronization occurs as a function of their diameter mismatch. We obtain numerically a phase diagram showing the transition between unsynchronized and synchronized states and compare it to analytical predictions we make using the Thiele approach. Our study demonstrates that for relatively small diameter differences the synchronization dynamics can be described qualitatively using Adler equation. However, when the diameters difference increases significantly, the system becomes strongly non-Adlerian. © *2013 AIP Publishing LLC*. [http://dx.doi.org/10.1063/1.4821073]

The study of synchronization processes is an important problem of nonlinear science, not only because of the wide range of applications in physics, biology, chemistry, and even in social systems, but also because of numerous fundamental challenges in understanding the collective dynamics of large ensembles. Recently, a great attention has been drawn to the studies of the phase locking in the arrays of Spin-Torque Nano-Oscillators (STNO).[1,2,34] STNOs benefit from the spin-transfer phenomenon[3–5] to generate the precession of magnetization in a free magnetic layer and magnetoresistance effects to get the corresponding voltage signal. These generators are nanoscaled, easily compatible with CMOS architectures, and can be easily tuned by dc current and/or external magnetic field.

Here, we consider STNOs whose free layers are in a vortex state, where the gyrotropic motion of vortex core can be excited by the injection of a dc current through a STNO stack, even without any applied external magnetic field.[6] Using both the gyrotropic vortex core motion and the tunnel magnetoresistance (TMR) it is possible to obtain coherent and high power output microwave signals.[7] Interest to synchronization of STNOs has arisen initially from the need to increase further the coherence of the magnetic oscillations to match the requirements of telecommunication applications, but is increasingly considered as a strong candidate for coherent multiple spin-wave emissions[8] as well as for networks of oscillators for associative memory applications.[9,10]

There are several remarkable experimental and theoretical studies of STNOs synchronization achieved by various physical mechanisms: Through electrical connection in series of STNOs,[11–13,35] by spin wave propagation,[14,15] and by antivortices,[16,17] another important mechanism to synchronize STNOs is the magnetostatic coupling.[18–22] The theoretical description of the synchronization dynamics of vortex STNO is more complicated than the well known oscillating systems such as coupled Van der Pol oscillators or rotators (Josephson junction, rotating pendula) which have fixed orbit radius, i.e., one degree of freedom, and thus can be described by the Adler equation.[23]

In this paper, we investigate the feasibility of synchronization through dipolar interaction focusing on the case of spin transfer vortex oscillators (STVOs). The vortex oscillator is a model system of particular interest since it only couples to neighbors due to the almost zero mean magnetization at equilibrium. The orbit radius in STVOs may change in time at the limit cycle, making their phase spaces multidimensional. Thus, the second aim is to understand the workability of simplified analytical descriptions based on Thiele equation for the synchronization dynamics studies.

We consider a system of two nanopillars (see Fig. 1), each composed by a free magnetic layer, a nonmagnetic spacer, and a fixed polarizer which generates a perpendicular spin polarization p_z. Free layers in both STVOs are $h = 10$ nm thick $Ni_{81}Fe_{19}$.[24] The initial magnetic configuration is two centered vortices with the same core polarities and chiralities. The polarizing layers are not included in our consideration because these layers, being uniformly magnetized in z direction, have almost no influence on the vortices motion.

In order to put STVOs in a steady oscillation regime, equal current densities J of 7×10^6 A/cm^2 with the identical spin polarization $p_z = 0.2$ which corresponds to spin-torque amplitude $a_J = 5$ Oe are injected through both STVOs. The difference in initial frequencies of the two oscillators f_1^i and f_2^i arise because of the deliberate pillar diameters difference $\Delta D = D_1 - D_2$ around a mean diameter $D_0 = 200$ nm. Such system simulates real device situations, when STVOs are not identical because of lithography process accuracy.

In this work, we have performed the series of micromagnetic simulations for diameters corresponding to differences between 2.5% and 15%. For each case, we varied interpillar

a)Electronic mail: konstantin.zvezdin@gmail.com

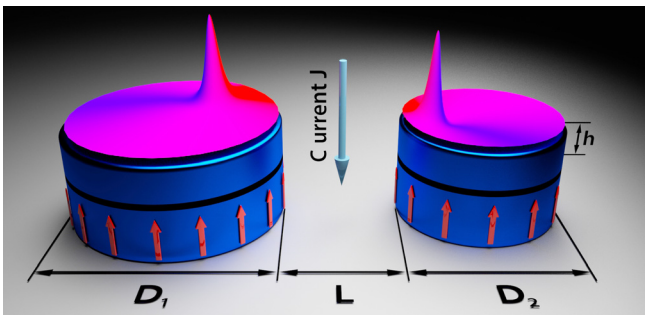

FIG. 1. Schematic representation of the studied system. There are two STNOs with diameters $D_{1,2} = D_0 \pm \Delta D/2$, where $D_0 = 200$ nm and $\Delta D/D_0$ ($\Delta D = D_1 - D_2$) is a diameters detuning which is not more than 15%.

TABLE I. Diameters difference and critical distance L_{cr} where synchronization still exists. Frequencies f_1^i and f_2^i correspond to the frequencies of isolated STVOs and f_{12} is the common frequency after synchronization.

D_1 (nm)	D_2 (nm)	$\Delta D/D_0$ (%)	L_{cr} (nm)	f_1^i (MHz)	f_2^i (MHz)	f_{12} (MHz)
202.5	197.5	2.5	607.5	473.1	480.6	477.8
205	195	5	495	469.4	484.7	484.7
207.5	192.5	7.5	397.5	465.4	488.9	469.8
210	190	10	287.5	462.2	493.7	468.1
212.5	187.5	12.5	150	458.0	498.0	463.5
215	185	15	90	457.0	501.9	456.5

distance with a step of 2.5 nm in order to determine the critical distance at which STVOs are still synchronized. The results of these simulations are summarized in Table I. In Figure 2(a)), we present the evolution of the spectrum of the M_x component of the magnetization with decreasing distance between disk edges for the case $D_1 = 210$ nm, $D_2 = 190$ nm. At interpillar distances $L > L_{cr}$, the spectrum contains two peaks at the frequencies of the two independent oscillators. When $L < L_{cr}$, the oscillators become synchronized and oscillate together at a single frequency f_{12}. The synchronized frequency f_{12} stands between the frequencies of the isolated STVOs, with a value closer to the frequency of the bigger oscillator. To illustrate the synchronization process, the core dynamics in the case $D_1 = 202.5$ nm, $D_2 = 197.5$ nm, and $L = 600$ nm ($L < L_{cr}$) are shown in Figs. 2(b) (core orbit radii X_1, X_2) and 2(c) (phase difference). As the vortices orbits increase towards their steady state values, the dipolar interaction between the vortices increases. Once the interaction energy becomes strong enough, a phase locking occurs, leading to convergence of the phase difference to a constant value.

High frequency oscillations of the orbit radii and the phase difference can be observed even after the synchronization is achieved (Figs. 2(b) and 2(c) insets). They are associated to high frequency forces acting on the cores in their gyrotropic rotating frame induced by the dipolar interaction. Notably, their action is averaged over the timescale of the synchronization process, and will be neglected in the development of our models.

Table I presents the evolution of the critical distance L_{cr} and the frequency of synchronized oscillators f_{12} with the diameter difference, compared to the isolated frequencies f_1^i and f_2^i. For diameters difference below 10%, we found that critical distances are greater than 250 nm, demonstrating the high efficiency of dipolar coupling for vortex oscillators synchronization. Mostly, these distances are easily compatible with standard lithography techniques.

In the theory of synchronization, the interaction between oscillators and the dynamics of the phase difference, in the simplest cases, can be described by Adler's equation[25]

$$\frac{d\psi}{dt} = \Delta\omega + u \sin\psi, \tag{1}$$

where $\Delta\omega$ is a difference between frequencies of oscillators and u is proportional to the interaction energy. In the plane of parameters $(\Delta\omega, u)$ the region $-u < \Delta\omega < u$ is the one where Eq. (1) has stable stationary solutions. This zone corresponds to phase locking and frequency entrainment and it is called Arnold tongue.[26]

We now seek a more detailed insight on the synchronization process starting from two coupled Thiele equations. These equations describe the vortices motions in their self-induced gyrotropic mode and include a spin-transfer term as well as a coupling term[27–30]

$$\begin{aligned} &G(\mathbf{e}_z \times \dot{\mathbf{X}}_{1,2}) - k_{1,2}(\mathbf{X}_{1,2})\mathbf{X}_{1,2} - \mathcal{D}_{1,2}\dot{\mathbf{X}}_{1,2} \\ &-\mathbf{F}_{STT1,2} - \mathbf{F}_{int}(\mathbf{X}_{1,2}) = \mathbf{0}, \end{aligned} \tag{2}$$

where $G = -2\pi p M_s h/\gamma$ is the gyroconstant, p is core polarity, and γ is the gyromagnetic ratio. The confining force is given with $k(\mathbf{X}_{1,2}) = \omega_{01,2} G\left(1 + a\frac{\mathbf{X}_{1,2}^2}{R_{1,2}^2}\right)$, where $R_{1,2}$ are disc radii[31,32] and the gyrotropic frequency is $\omega_{01,2} = \frac{20}{9}\gamma M_s h/R_{1,2}$. In this study, the Oersted field influence on the dynamics was not taken into account, since at first order it will only shift the self-frequencies of the vortex oscillators and have no influence on the synchronization process. The damping coefficient—$\mathcal{D}_{1,2} = \alpha\eta_{1,2}G$, $\eta_{1,2} = \frac{1}{2}\ln\left(\frac{R_{1,2}}{2l_e}\right) + \frac{3}{8}$,

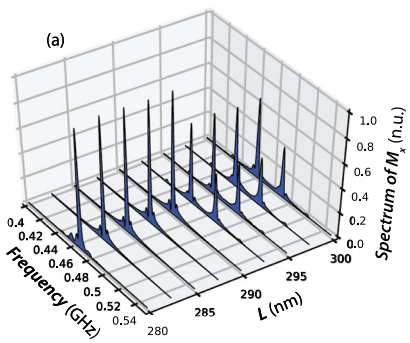

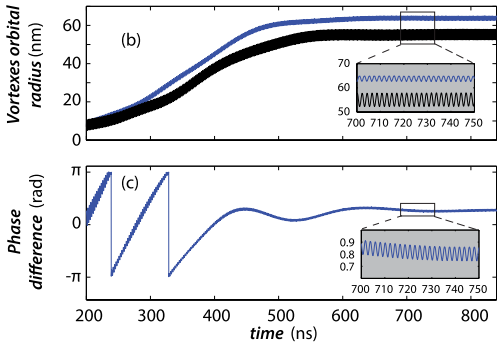

FIG. 2. (a) Power spectrum density of x-component of total magnetization as a function of distance between disks edges for $\Delta D/D_0 = 10\%$, showing the transition between unsynchronized and synchronized states. (b) Core positions $X_{1,2}$ vs time for $\Delta D/D_0 = 2.5\%$, $L = 600$ nm. (c) Phase difference as a function of time, ($\Delta D/D_0 = 2.5\%$, $L = 600$ nm).

where $l_e = \sqrt{\frac{A}{2\pi M_s^2}}$. The fourth term $\mathbf{F}_{STT1,2}$ is the spin transfer force. For the case of uniform perpendicularly magnetized polarizers $\mathbf{F}_{STT1,2} = \pi\gamma a_J M_s h(\mathbf{X}_{1,2} \times \mathbf{e}_z) = \varkappa(\mathbf{X}_{1,2} \times \mathbf{e}_z)$ (see Ref. 28), where the spin torque coefficient is $a_J = \hbar p_z J/(2|e|hM_s)$, $\hbar$ is the Planck's constant, and e is the elementary charge. We chose to apply an equal current density through the two pillars to ensure identical spin transfer forces on the two vortex cores.

The interpillar interaction is summarized by a dipolar coupling force term: $\mathbf{F}_{int}(\mathbf{X}_{1,2}) = -\mu(L)\mathbf{X}_{2,1}$, where $\mu(L)$ is a coupling parameter depending on the interpillar distance. Here, only the first order interactions are considered in keeping with previous work.[30] Since small variations of disc diameter do not cause significant changes of dipolar coupling parameter $\mu(L)$, we can fairly estimate it from the results obtained for the case of identical diameters in Ref. 30. The Arnold tongue (the region in the plane $(\Delta D/D_0, \mu(L))$ for which synchronization is achieved), extracted with the full micromagnetic simulations is shown in Fig. 3, as the shaded region limited by dashed line with empty squares.

Using the coupled equations, we now aim to deduce a simple Adler-like equation describing the synchronization process. In polar coordinates $(X_{1,2}\cos\varphi_{1,2}, X_{1,2}\sin\varphi_{1,2})$ Eq. (2) reads

$$\frac{\dot{X}_1}{X_1} = \alpha\eta_1\dot{\varphi}_1 - \frac{\varkappa}{G} + \frac{\mu}{G}\frac{X_2}{X_1}\sin(\varphi_1 - \varphi_2), \tag{3a}$$

$$\dot{\varphi}_1 = -\frac{k(X_1)}{G} - \alpha\eta_1\frac{\dot{X}_1}{X_1} - \frac{\mu}{G}\frac{X_2}{X_1}\cos(\varphi_1 - \varphi_2), \tag{3b}$$

$$\frac{\dot{X}_2}{X_2} = \alpha\eta_2\dot{\varphi}_2 - \frac{\varkappa}{G} - \frac{\mu}{G}\frac{X_1}{X_2}\sin(\varphi_1 - \varphi_2), \tag{3c}$$

$$\dot{\varphi}_2 = -\frac{k(X_2)}{G} - \alpha\eta_2\frac{\dot{X}_2}{X_2} - \frac{\mu}{G}\frac{X_1}{X_2}\cos(\varphi_1 - \varphi_2). \tag{3d}$$

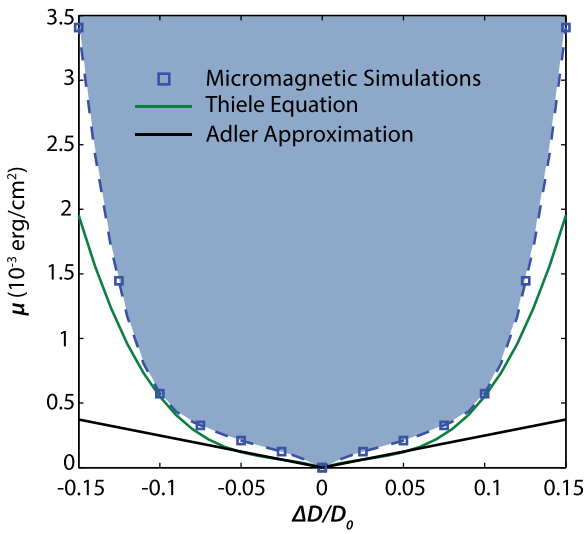

FIG. 3. Arnold tongues obtained by micromagnetic simulations (shaded region limited by blue squares), by numerical solutions of Eqs. (3a)–(3d) (green line), and by Adler approximation (black line). The inner part of the tongue represents synchronization region.

We can make some simplifications for small diameter differences $(\Delta D/D_0 < 0.05)$: (a) The condition $\Delta D/D_0 \ll 1$ allows us to linearize the following terms as

$$k_{1,2}(X_{1,2}) \approx G\left[\omega_0\left(1 \mp \frac{1}{2}\frac{\Delta D}{D_0}\right) + \omega_0 a\frac{X_{1,2}^2}{R_0^2}\left(1 \mp \frac{3}{2}\frac{\Delta D}{D_0}\right)\right],$$

$$\eta_{1,2} \approx \eta_0 \pm \frac{1}{4}\frac{\Delta D}{D_0},$$

where ω_0 and η_0 are the gyrotropic frequencies for a disc with radius $R_0 = 100\,\text{nm}$ and the damping $\eta_0 = \frac{1}{2}\ln\left(\frac{R_0}{2l_e}\right) + \frac{3}{8}$. (b) Assuming that the steady state vortex radii hardly differs from its mean value, we can write $X_{1,2} = X_0(1 \pm \varepsilon)$, where $X_0 = (X_1 + X_2)/2 = 60\,\text{nm}$ (this value was obtained by micromagnetic simulations for the case of same diameters with $D_0 = 200\,\text{nm}$), and $\varepsilon = (X_1 - X_2)/(X_1 + X_2) \ll 1$ at the limit cycle. This assumption was confirmed by micromagnetic modeling for small $\Delta D/D_0$. (c) The synchronization of STVOs with small diameters difference appears on large interpillar distances, on these distances the interaction between disks is quite weak and we can say that $\mu \ll G\omega_0 a r_0^2$, where $r_0 = X_0/R_0$ (our calculations showed that for $L > 400\,\text{nm}$ $\mu \sim 10^{-4}\,\text{erg/cm}^2$ and $G\omega_0 a r_0^2 \sim 0.1\,\text{erg/cm}^2$).

These approximations allow us to transform Eqs. (3a)–(3d) to the second order differential equation for phase difference $\psi = \varphi_1 - \varphi_2$

$$\frac{1}{2a\omega_0 r_0^2}\ddot{\psi} + \alpha\eta_0\dot{\psi} + 2\frac{\mu}{G}\sin\psi = \frac{1}{2}\alpha\frac{\Delta D}{D_0}\omega_0(1 + ar_0^2). \tag{4}$$

At the limit cycle the second derivative of ψ in Eq. (4) tends to zero. The equation of motion then reads

$$\frac{\mathrm{d}\psi}{\mathrm{d}t} = \frac{1 + ar_0^2}{2\eta_0}\frac{\Delta D}{D_0}\omega_0 - \frac{2\mu}{G\alpha\eta_0}\sin\psi. \tag{5}$$

Equation (5) has the stationary solutions when

$$|\mu| \le G\frac{\alpha}{4}(1 + ar_0^2)\frac{\Delta D}{D_0}\omega_0.$$

The synchronization region for Eq. (5) is added in Fig. 3 (black line). It is seen that when $\Delta D/D_0 \ge 5\%$ the boundary values obtained from Adler-like Eq. (5) differs from micromagnetic simulations even qualitatively. Therefore, our linearization cannot be extended to the cases of significant diameter mismatch. To complete our study and capture such strongly asymmetric regimes, we finally evaluate the validity of the coupled Thiele equations, without the latter approximations, to describe the synchronization dynamics.

Equations (3a)–(3d) were solved numerically using coupling parameter μ derived from micromagnetic simulations[30] and the corresponding phase-diagram extracted (green line in Fig. 3). As can be seen, Eqs. (3a)–(3d) give us reliable results for diameters difference bigger than 5%, further than with the simple Adler-like approach.

With the further increase of diameter difference, the mismatch between the results obtained using Eqs. (3a)–(3d) and the ones derived from micromagnetic simulations

becomes more significant. These differences come from the fact that the Thiele equation was initially developed to describe the steady oscillation regime with unperturbed orbit radius.[29,33] Therefore our equations cannot perfectly describe the core dynamics when perturbed by a dipolar interaction, especially when the eigenfrequency difference between oscillators is large. However, this approach describes the synchronization process well for the diameter differences up to 12% much more than standard error of state-of-the-art fabrication process.

In summary, we have shown the possibility to synchronize two STVOs with a frequency difference due to a difference in pillar diameter. Our micromagnetic simulations have shown that the phase locking of this system appears at inter-pillar distances below a critical value L_{cr} which depends on diameter difference $\Delta D/D_0$. We have obtained the phase diagram (Arnold tongue) which demonstrates the transition between synchronized and unsynchronized regions. We have also provided a quantitative analytical treatment based on Thiele equations. Our study has shown that for $\Delta D/D_0 \leq 5\%$, the synchronization phase diagram can be described qualitatively using an Adler-like equation (5). However, the system becomes strongly non-Adlerian once the diameter exceeds 5%. Although further increase of diameters difference drives the synchronization dynamics into non-Adlerian regime, it can still be well described by numerical integration of non-linearized Thiele equations. Only for very large diameter differences (more than 12%), which is far above the typical error in state-of-the-art fabrication processes, does the Thiele-based approach fail to describe the synchronization process. The reason for the increasing complexity of synchronization regimes in strongly asymmetric systems might be the excitation of strongly nonlinear modes.

The authors thank Alexey V. Khvalkovskiy and Lee C. Phillips for helpful discussions. The work was supported by RFBR Grant Nos. 10-02-01162 and 11-02-91067, CNRS PICS Russie No. 5743 2011, Dynasty Foundation, and the ANR agency (SPINNOVA ANR-11-NANO-0016) and EU FP7 Grant (MOSAIC No. ICT-FP7-n.317950). F.A.A. acknowledges the Research Science Foundation of Belgium (FRS-FNRS) for financial support (FRIA Grant).

[1]V. Tiberkevich, A. Slavin, E. Bankowski, and G. Gerhart, Appl. Phys. Lett. **95**, 262505 (2009).
[2]H. Jung, K.-S. Lee, D.-E. Jeong, Y.-S. Choi, Y.-S. Yu, D.-S. Han, A. Vogel, L. Bocklage, G. Meier, M.-Y. Im, P. Fischer, and S.-K. Kim, Sci. Rep. **1**, 59 (2011).
[3]J. C. Slonczewski, J. Magn. Magn. Mater **195**, 261 (1999).
[4]L. Berger, Phys. Rev. B **54**, 9353 (1996).
[5]S. Kiselev, J. C. Sankey, I. N. Krivorotov, N. C. Emley, R. J. Schoelkopf, R. A. Buhrman, and D. C. Ralph, Nature **425**, 380 (2003).
[6]F. Abreu Araujo, M. Darques, K. A. Zvezdin, A. V. Khvalkovskiy, N. Locatelli, K. Bouzehouane, V. Cros, and L. Piraux, Phys. Rev. B **86**, 064424 (2012).
[7]A. Dussaux, B. Georges, J. Grollier, V. Cros, A. V. Khvalkovskiy, A. Fukushima, M. Konoto, H. Kubota, K. Yakushiji, S. Yuasa, K. A. Zvezdin, K. Ando, and A. Fert, Nature Commun. **1**, 8 (2010).
[8]V. E. Demidov, S. Urazhdin, and S. O. Demokritov, Nature Mater. **9**, 984–988 (2010).
[9]G. Csaba, M. Pufall, W. Rippard, and W. Porod, in *Proceedings of the 12th IEEE International Conference on Nanotechnology (IEEE-NANO)* (2012), pp. 1–4.
[10]A. Horváath, F. Corintoz, G. Csaba, W. Porod, and T. Roska, in *Proceedings of the 13th International Workshop on Cellular Nanoscale Networks and Their Applications (CNNA)* (2012), pp. 1–4.
[11]B. Georges, J. Grollier, M. Darques, V. Cros, C. Deranlot, B. Marcilhac, G. Faini, and A. Fert, Phys. Rev. Lett. **101**, 017201 (2008).
[12]B. Georges, J. Grollier, V. Cros, and A. Fert, Appl. Phys. Lett. **92**, 232504 (2008).
[13]J. Grollier, V. Cros, and A. Fert, Phys. Rev. B **73**, 060409(R) (2006).
[14]X. Chen and R. H. Victora, Phys. Rev. B **79**, 180402 (2009).
[15]D. V. Berkov, Phys. Rev. B **87**, 014406 (2013).
[16]C. E. Zaspel, Appl. Phys. Lett. **102**, 052403 (2013).
[17]A. Ruotolo, V. Cros, B. Georges, A. Dussaux, J. Grollier, C. Deranlot, R. Guillemet, K. Bouzehouane, S. Fusil, and A. Fert, Nat. Nanotechnol. **4**, 528 (2009).
[18]J. Shibata, K. Shigeto, and Y. Otani, Phys. Rev. B **67**, 224404 (2003).
[19]A. Vogel, A. Drews, T. Kamionka, M. Bolte, and G. Meier, Phys. Rev. Lett. **105**, 037201 (2010).
[20]A. A. Awad, G. R. Aranda, D. Dieleman, K. Y. Guslienko, G. N. Kakazei, B. A. Ivanov, and F. G. Aliev, Appl. Phys. Lett. **97**, 132501 (2010).
[21]S. Barman, T. Kimura, Y. Fukuma and Y. Otani, J. Phys. D **43**, 422001 (2010).
[22]H. Jung, Y.-S. Yu, K.-S. Lee, M.-Y. Im, P. Fischer, L. Bocklage, A. Vogel, M. Bolte, G. Meier, and S.-K. Kim, Appl. Phys. Lett. **97**, 222502 (2010).
[23]A. Pikovsky, M. Rosenblum, and J. Kurths, *Synchronization: A Universal Concept in Nonlinear Sciences* (Cambridge University Press, Cambridge, 2001).
[24]The magnetic parameters of the free layers are: The magnetization $M_s = 800$ emu/cm^3, the exchange constant $A = 1.3 \times 10^{-6}$ erg/cm, and the damping parameter $\alpha = 0.01$. The micromagnetic simulations have been performed by numerical integration of the Landau-Lifshitz-Gilbert equation using our micromagnetic code SpinPM based on the fourth order Runge-Kutta method with an adaptive time-step control for the time integration and a mesh size 2.5×2.5 nm^2.
[25]R. Adler, Proc. IRE **34**, 351 (1946).
[26]V. I. Arnold, Chaos **1**, 20 (1991).
[27]A. A. Thiele, Phys. Rev. Lett. **30**, 230 (1973).
[28]A. V. Khvalkovskiy, J. Grollier, A. Dussaux, K. A. Zvezdin, and V. Cros, Phys. Rev. B **80**, 140401 (2009).
[29]Y. Gaididei, V. P. Kravchuk, and D. D. Sheka, Int. J. Quantum Chem. **110**, 83 (2010).
[30]A. D. Belanovsky, N. Locatelli, P. N. Skirdkov, F. Abreu Araujo, J. Grollier, K. A. Zvezdin, V. Cros, and A. K. Zvezdin, Phys. Rev. B **85**, 100409 (2012).
[31]K. Y. Guslienko, X. F. Han, D. J. Keavney, R. Divan, and S. D. Bader, Phys. Rev. Lett. **96**, 067205(R) (2006).
[32]B. A. Ivanov and C. E. Zaspel, Phys. Rev. Lett. **99**, 247208 (2007).
[33]B. A. Ivanov, G. G. Avanesyan, A. V. Khvalkovskiy, N. E. Kulagin, C. E. Zaspel, and K. A. Zvezdin, JETP Lett. **91**, 178 (2010).
[34]O. V. Sukhostavets, J. González, and K. Y. Guslienko, Phys. Rev. B **87**, 094402 (2013).
[35]Y. Zhou, V. Tiberkevich, G. Consolo, E. Iacocca, B. Azzerboni, A. Slavin, and J. Åkerman, Phys. Rev. B **82**, 012408 (2010).